Arrangement of dermal chromatophore units in a polymorphic species,

Ranitomeya imitator

By

Mallory de Araujo Miles

December 2021

Director of Thesis: Kyle Summers, PhD

Major Department: Biology

In the 1980s, Rainer Schulte became the first to describe a species of poison frog living in the Amazon rainforest: *Ranitomeya imitator.* Schulte's classification of *R. imitator* as a single species sparked immediate controversy , since the species is composed of several dispersed populations, each exhibiting a unique color pattern (Caldwell 1990). The phenotypic differences apparent to even a casual observer of the *R. imitator* complex beg the question: how different are these frogs beneath their colorful skin? The present study attempts to quantify histological differences between the four color morphs of *R. imitator* and to demonstrate that the most closely related morphs have the most similar histology. Two types of chromatophores—melanophores and xanthophores—were measured in over 2,000 images of integumentary tissue taken under a brightfield microscope. One-way ANOVA tests were used to compare the abundance of chromatophores in skin tissue of different colors and from different morphs. Black tissue was found to exclusively contain melanophores, and melanophore abundance varied little between color morphs. Yellow and orange tissue contained a combination of xanthophores and melanophores. Xanthophores were most abundant in orange tissue from the banded morph, followed by the varadero morph, then the striped morph. Melanophore abundance followed the

opposite trend. Green skin tissue (from the striped and spotted morphs) contained fewer xanthophores and more melanophores than orange tissue. Histological differences observed in this study correspond with the timing of mimetic divergence events proposed by Twomey et al. 2016, suggesting that differences have accumulated in the morphs since their divergence (Twomey 2016). Additionally, poison glands were measured to determine whether any color morph might have greater capacity for sequestering alkaloid toxins than another. Significant statistical differences in poison gland abundance existed between three of the four color morphs. The varadero morph exhibited the greatest abundance of poison glands, in contrast to findings from previous field studies in which the varadero morph exhibited relatively low alkaloid content. This discrepancy suggests that alkaloid defenses may be influenced more by dietary availability of alkaloids than poison gland storage capacity. Furthermore, the banded morph, which exhibits the brightest aposematic colors, and the spotted morph, which exhibits the least bright colors, showed no significant differences in poison gland abundance, suggesting that variation in aposematic signal intensity across color morphs may not be quantitatively honest. Together, the histological differences found in this study provide another piece of evidence to support the hypothesis that persistent color polymorphism may indicate an early stage of speciation in the mimic poison frog, *Ranitomeya imitator*.

Arrangement of dermal chromatophore units in a polymorphic species, *Ranitomeya imitator*

A Thesis

Presented to the Faculty of the Department of Biology

At East Carolina University

in Partial Fulfillment of the Requirements for the Degree

Master of Science in Biology

By

Mallory de Araujo Miles

December 2021

© Mallory de Araujo Miles, 2021

Arrangement of dermal chromatophore units in a polymorphic species, *Ranitomeya imitator*

By

Mallory de Araujo Miles

APPROVED BY:

DIRECTOR
OF THESIS: _____
Kyle Summers, PhD

COMMITTEE
MEMBER: _____
Jeffrey McKinnon, PhD

COMMITTEE
MEMBER: _____
Timothy Erickson, PhD

CHAIR OF THE
DEPARTMENT
OF BIOLOGY: _____
David Chalcraft, PhD

DEAN OF THE
GRADUATE SCHOOL: _____
Paul Gemperline, PhD

ACKNOWLEDGEMENTS

First and foremost, I would like to offer my gratitude to my advisor, Dr. Kyle Summers, for giving me the opportunity to study an organism that has fascinated me since childhood and for helping me fit that organism into broader concepts of ecology and evolution. Without Dr. Summers, this work would not have been possible. I would also like to thank my committee members, Dr. Trip Lamb, Dr. Jeffrey McKinnon, and Dr. Timothy Erickson for their support and feedback throughout the evolution of this project. I would like to thank my lab member, Andrew Rubio, for keeping the lab running smoothly, and my colleague, Jasper Leavitt, for assisting me with statistical analysis. Finally, I am thankful to my friends and family, whose support helped give me the stamina to complete this project.

TABLE OF CONTENTS

LIST OF TABLES

LIST OF FIGURES

INTRODUCTION

Color polymorphism

The phenomenon of color polymorphism (the persistence of multiple, discrete color phenotypes in a single population or species) has long held the interest of ecologists and evolutionary biologists. Because color plays a vital role in many life processes, including crypsis, aposematism, sexual signaling, and thermoregulation, optimal color patterns should quickly become fixed within a species, and color polymorphism should be a rare occurrence in nature. However, examples of color polymorphism can be found in most major groups of multicellular animals, as well as gymnosperm and angiosperm plants (White 2016). The unexpected prevalence of color polymorphism suggests the phenomenon may have ecological significance. Examining the mechanisms of color polymorphism may provide a window into a species' response to environmental change and, perhaps, into the early stages of speciation.

The mimic poison frog, *Ranitomeya imitator,* is a small dendrobatid frog native to Peru. Like many poison frogs, *R. imitator* uses bright aposematic colors to signal its toxicity to potential predators. *Ranitomeya imitator* has recently undergone a mimetic radiation event, producing a striking example of color polymorphism. The species includes four discrete color morphs—varadero, striped, spotted, and banded—across its geographic range. Each of these morphs corresponds with a sympatric congener: *R. fantastica, R. variabilis* highland, *R. variabilis* lowland, and *R. summersi* respectively (Twomey 2016).

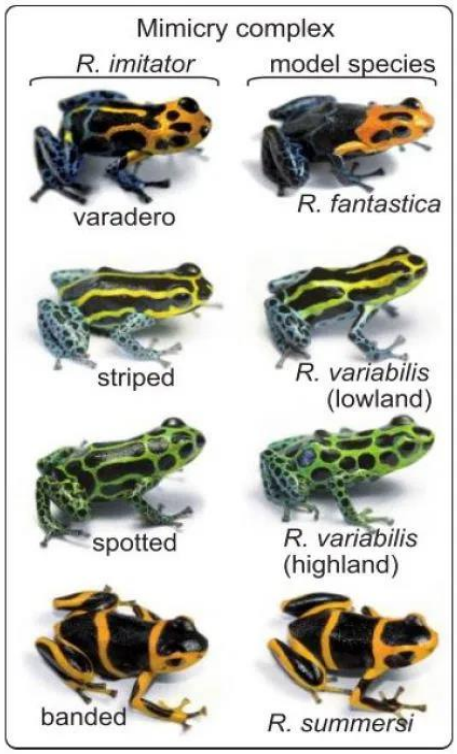

Figure 1. Four color morphs of the mimetic frog R. imitator and their congener models. (Twomey 2016)

The persistence of the four color morphs can be explained by Müllerian mimicry (Saporito 2006). Each morph benefits from taking on a different color pattern because that color pattern resembles another noxious species sharing the same geographic space. The shared color pattern triggers reciprocal learned avoidance in local predators; a predator who has been exposed to an unpalatable mimic will, in the future, avoid preying upon the model and vice versa. Empirical studies have confirmed that avian predators of *R. imitator* are capable of learning regionally-specific aposematic signals but are less successful at recognizing novel signals. For example, a banded *R. imitator* in the range of *R. summersi* is less likely to be predated than a striped *R. imitator* in the same range. Natural selection favors the persistence of the banded morph within the range

of *R. summersi*, in keeping with the predictions of Müllerian mimicry (Stuckert 2014, Yeager 2012).

The distinctions between the four color morphs may also be reinforced by sexual selection. Mate-choice experiments staged in a transition zone between the ranges of the striped and varadero morphs have supplied evidence for assortative mating, with striped males from the transition zone preferring to mate with striped females over varadero females (Twomey 2014). Over time, this preference could drive the two populations towards phenotypic extremes and reduce the fitness of intermediate phenotypes. Some studies have suggested that the preference could eventually develop into a reproductive barrier (Stuckert 2020, Symula 2001, Twomey 2014).

Because color pattern in *R. imitator* is subject to divergent selection through predation and contributes to non-random mating, color pattern can be considered a 'magic trait.' Magic traits are noted for their ability to drive speciation in populations that are still connected by gene flow (Servedio 2011, Stuckert 2020). Thus, differences in color pattern—and the underlying mechanisms that produce color pattern—may represent more than just fixed local optima. They may be an example of an association between color polymorphism and speciation at an early stage.

Color production

Most color production mechanisms in vertebrates can be categorized either as structural or pigmentary. Structural mechanisms produce bright colors, often blues and greens, by reflecting light off nanoscale structures found in the integument. By contrast, pigments produced by specialized cells in the dermis absorb light of a specific wavelength, leaving the remaining wavelengths of light visible to an observer (Mills 2008). Structural mechanisms and pigmentary mechanisms frequently interact to produce colors of varying hue and brilliance (Segami 2017).

Amphibians use specialized cells called chromatophores to produce color. Chromatophores are generally found layered within the dermal and subdermal tissue. Chromatophore layers are usually found in close contact with each other and are frequently referred to as chromatophore units (Dushane 1935). The most superficial chromatophore, the xanthophore, contains pteridine and/or carotenoid pigments. These pigments absorb violet, blue, and green light to produce yellow, orange, and red coloration. Iridophores may be found below xanthophores. Iridophores contain nanoscale guanine platelets that reflect light; traditionally, they have been associated with the production of bright blue and green coloration, although more recently they have been associated with a broader color spectrum. When found beneath xanthophores, iridophores may also increase the brightness of superficial colors (Shawkey 2005, Shawkey 2017, Twomey 2020). The deepest chromatophore, the melanophore, contains eumelanin or pheomelanin pigments. These pigments absorb most of the light in the visible spectrum and produce dark brown or black coloration (Dushane 1935, Frost 1984). When found below iridophores, melanophores may enhance blue or green colors by absorbing stray light scattered incoherently by the guanine platelets (Shawkey 2017).

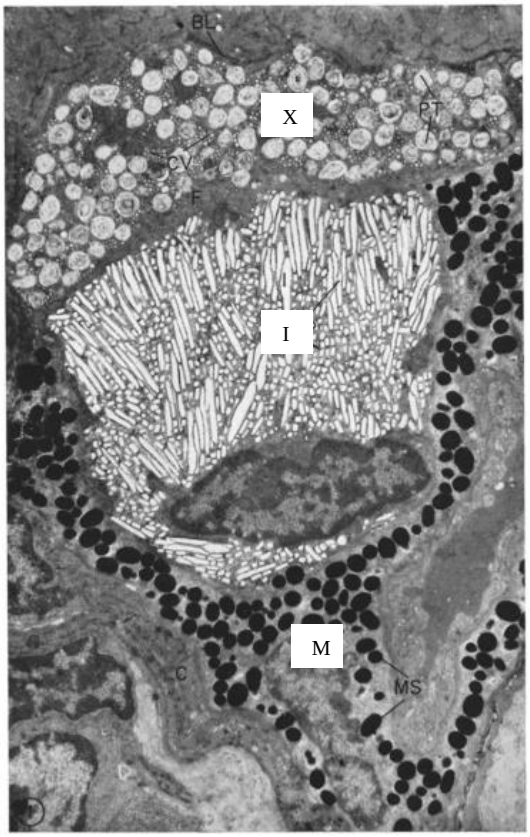

Figure 2. Electron micrograph of skin section from H. cinerea, *showing a dermal chromatophore unit. A xanthophore (X) with multiple carotenoid vesicles and pteridine vesicles is shown at the surface of the chromatophore unit. An iridophore (I) with reflective platelets appears below the xanthophore. A melanophore (M) with multiple melanosomes wraps around the iridophore. (Bagnara 1968)*

Recent studies have begun to describe chromatophore units in *R. imitator* and some of its model species. The usual vertebrate chromatophores—melanophores, xanthophores, and iridophores—are all present in *R. imitator* and its models, suggesting that their shared phenotype is produced by homologous structures. However, *R. imitator* shows a higher level of variability in chromatophore arrangement than other dendrobatid species. This variability may have allowed for the rapid diversification of *R. imitator* into distinct color morphs (Twomey 2020).

Toxin sequestration

Dendrobatid frogs are a textbook example of aposematism, using bright colors to warn predators that they are unpalatable or even dangerous to consume. While dendrobatid frogs produce most of their colors endogenously, they obtain alkaloid toxins exogenously, by consuming ants and mites and sequestering alkaloid toxins from these prey items in specialized granular glands in their dermal tissue.

Despite their popularity as representatives of aposematism, the honesty of aposematic signals in dendrobatid frogs has recently been called into question. A significant amount of interspecific and intraspecific variation exists in the toxicity levels of dendrobatid frogs and in the brightness of their aposematic signals. Higher toxicity levels do not always correlate with brighter aposematic signals (Stuckert 2018, Yang 2019). A number of hypotheses have arisen to describe the observed variation in toxicity in poison frogs (Table 3). Most focus on determining whether variation in toxicity is better explained by variation in access to dietary sources of alkaloids or variation in innate mechanisms for processing and storing alkaloids. Additionally, many studies attempt to determine whether toxicity levels can be positively correlated with brightness of aposematic signals, making these signals quantitatively honest in dendrobatid frogs. At the present moment, the scientific literature lacks a consensus on both of these questions.

Study objectives

The present study processes skin sections from the four morphs of *Ranitomeya imitator*. The abundance of melanophores, xanthophores, and poison glands is compared across skin sections of different colors and from different morphs. The study aims to address two main questions: 1) are significant histological differences present in the integumentary system of frogs of different color

morphs and 2) can the observed histological differences be correlated with the timing of divergence of the color morphs? If so, the accumulation of anatomical differences in *R. imitator* frogs of different color morphs after divergence may be consistent with an early stage of speciation. Additionally, the study determines whether poison gland abundance varies between color morphs of *R. imitator*. These findings are used to evaluate multiple hypotheses currently found in the scientific literature about the mechanisms of variation in toxicity among poison frogs and the quantitative honesty of aposematic signals in poison frogs.

METHODS

Captive frog colony

A captive colony of *R. imitator* frogs was established by procuring individuals from Understory Enterprises, a licensed supplier. These individuals were bred from frogs from known localities in Peru. The colony was established in 2011 and, to date, the frog colony consists of those frogs procured from Understory Enterprises as well as their offspring, bred by members of the Summers lab. The frog colony is maintained in a temperature-controlled room in the basement of Howell Science Complex at East Carolina University. The lights in the room are kept on a 12-hour light-dark cycle to maintain regular circadian rhythms, in accordance with the diurnal habits of *R. imitator*. Adult frogs are kept in vivaria containing sphagnum moss as substrate, pothos plants as foliage, and a coconut husk hide. Vivaria containing breeding pairs also contain two capped PVC pipes with water, which serve as egg deposition sites. Frog vivaria are misted regularly to maintain proper humidity. Adult frogs are fed ~10-15 wingless fruit flies each, 3 times per week. Tadpoles are fed tropical fish food twice a week, and once metamorphosed, small juveniles are fed a constant diet of springtails until they become large enough to consume fruit flies. Fruit fly and springtail populations are maintained within the lab. All animal use procedures necessary for this study were approved by the Institutional Animal Care and Use Committee at East Carolina University (AUP D281b).

Slide preparation

Twenty-four adult individuals were sacrificed using benzocaine gel applied to the venter, according to the AUP D281b. Of these individuals, six belonged to a varadero pedigree line

(VAO1, VAO2, VAO3, VAO4, VAO5, VAO6), six belonged to a striped pedigree line (PO16, PC22, PC23, PC24, PC25, PC26), six belonged to a spotted pedigree line (TUO4, TUO5, TUO6, 3701, 3703, 3704), and six belonged to a banded pedigree line (SA01, SA02, SA03, SA04, SA05, SA06). Immediately after the individuals were sacrificed, their dorsal skins were removed using micro-scalpels and a light microscope. Skins were dissected to separate regions of different colors, which were labeled as black, yellow, orange, or green. Skin sections of approximately 2 x 1 mm were collected from the separated regions. Skin sections were fixed in a 10% phosphate buffered formalin solution for 6-12 hours, then run through several dehydrating and clearing solvents in a tissue processor. Finally, a rotary microtome was used to embed the skins in paraffin wax, section them into sections with a thickness of 5µm, and fix the sections to glass microscope slides. A total of approximately 1,000 slides were produced, each slide containing 8-10 skin sections. This work was undertaken by previous Summers lab member, Adam Stuckert.

Histological staining

Histological slides were stained according to the Schmorl-Melanin protocol, which was designed to identify sites of melanin deposition. Each slide was dipped in a series of reagents, detailed in Table 1. Slidebrite and ethanol solutions were changed at the earliest sign of cloudiness or discoloration. Nuclear fast red and ferricyanide solutions were changed weekly. A plastic basket was developed so five slides could be submerged in reagent at a time, increasing the efficiency of slide processing.

Reagent	Time in Reagent	Purpose of Reagent
Slidebrite	3 minutes, 3 changes	deparaffinize tissue sections
100% ethanol	10 dips (~1 min), 2 changes	re-hydrate tissue

95% ethanol	10 dips (~1 min), 2 changes	re-hydrate tissue
Distilled water	15 seconds	rinse away any debris or residue
Ferricyanide solution (10 mL 1% potassium ferricyanide: 30 mL 1% ferric chloride)	1.5 minutes	stain melanin deposits black
Distilled water	15 seconds	rinse away excess ferricyanide solution
Nuclear fast red solution	5 minutes	stain cell nuclei red and surrounding tissue pink
Distilled water	15 seconds	rinse away excess nuclear fast red
95% ethanol	2 dips	dehydrate tissue
100% ethanol	2 dips	dehydrate tissue
Slidebrite	10 dips (~1 min), 3 changes	clear any non-specific stains
Permount mounting medium	indefinite	fix stains in tissue and adhere cover slip to slide

Table 1. Reagents used in histological staining. Reagents were specified by Newcomer's Schmorl Melanin Staining Protocol and exposure times were modified for optimal staining of R. imitator *tissue.*

Microscopy

Histological slides were examined under a brightfield microscope connected to a computer with digital display. A magnification strength of 40X was used to collect images. The first, fifth, and last skin section from each slide were selected for imaging, except when tissue degradation made a section unusable (gaps in tissue exceeded width of epidermis). When one section was deemed inviable, the nearest viable section was selected for imaging.

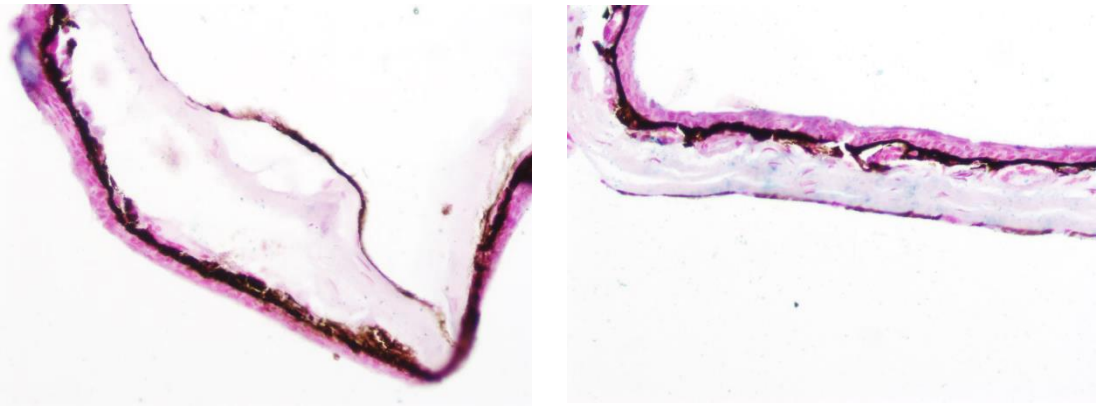

Figure 3. Left – degraded tissue section, excluded from the study. Right – intact tissue section, used in the study.

Skin sections on the same slide were assumed to be roughly equivalent, since they represent tissue of the same color taken from the same frog of the same morph at the same depth. Automatic white balance and exposure times were used to collect images. A total of 2072 images were produced.

Image analysis

Images were analyzed using ImageJ Software. A Bamboo stylus was used to outline regions of different cell types, and the area of each region (in pixels) was calculated. In some cases, several discrete regions had to be added together to find the total area of a given cell type.

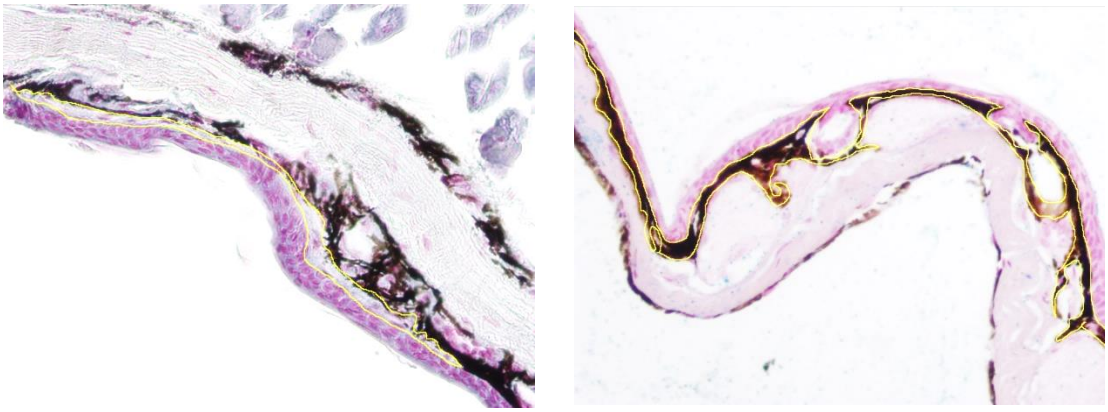

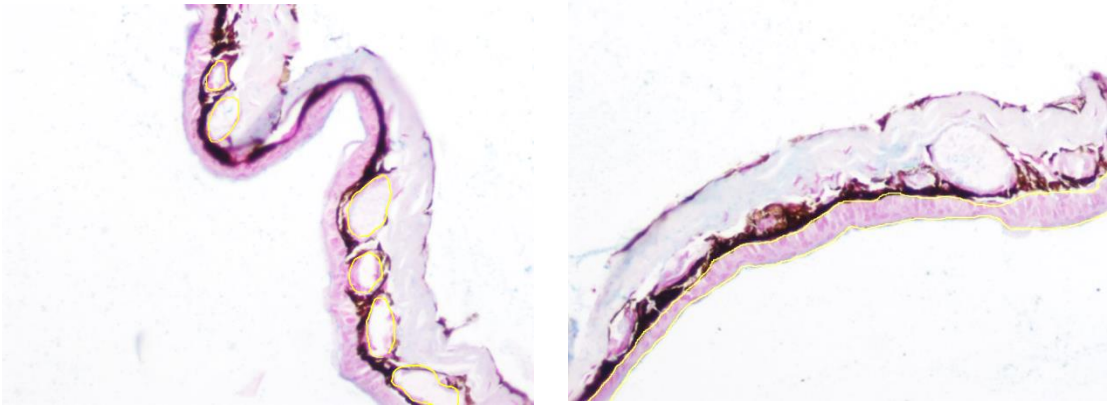

Figure 4. Regions of xanthophores (upper left), melanophores (upper right), poison glands (lower left), and epidermis (lower right) outlined in yellow.

Regions of dark brown or black pigmentation below the epidermis but above the dermis were considered to be melanophores. Regions of translucent cellular material with interspersed nuclei between the epidermis and the melanophores were considered to be xanthophores. Round regions of empty vesicles between the epidermis and the dermis were considered to be poison glands (Frost 1984). The pale region with parallel fibers was considered to be dermal tissue, and the pink region with densely crowded nuclei was considered to be epidermal tissue.

Statistical analysis

Measurements obtained from ImageJ analysis (total area of skin section, area of melanophores, area of xanthophores, area of poison glands) were entered into an Excel spreadsheet. Abundance of each cell type was calculated by dividing area of the cell type by total area of the skin section. Following these calculations, the Excel spreadsheet was imported into SAS Enterprise Guide 7.1.

Although the data set generated by the present study was large (2072 images were measured), not all the data points could be considered independent samples (24 adult frogs provided all skin sections imaged). A hierarchical relationship exists between the four color morphs and the six frogs from each color morph that were sampled. In order to manage the hierarchical nature of the data set, measurements taken from each individual frog were averaged and averages were compared to each other in a one-way ANOVA test, since the averages could be treated as independent samples. For example, forty-two measurements of melanophore abundance in black skin tissue were taken from the frog PC22. These measurements could not be considered independent samples because they came from the same frog. Forty-five measurements of melanophore abundance in black skin tissue were taken from the frog PC23. Again, these measurements could not be considered independent samples because they came from the same frog. However, the average of measurements from frog PC22 and the average of measurements from frog PC23 could be considered independent samples because they came from different frogs. Thus, average data was compared in the one-way ANOVA test.

The one-way ANOVA tests run within SAS Enterprise Guide 7.1 compared the variance observed between six individual frogs of the same color morph (within group variance) to the variance between frogs from different color morphs (between group variance) to test the null hypothesis that color morph has no effect on chromatophore abundance (or that all color morphs belong to the same statistical group). An F-value was produced to indicate how different the color morphs were, and a P-value was produced to indicate the likelihood of that level of difference being observed between color morphs if color morph had no effect on chromatophore abundance.

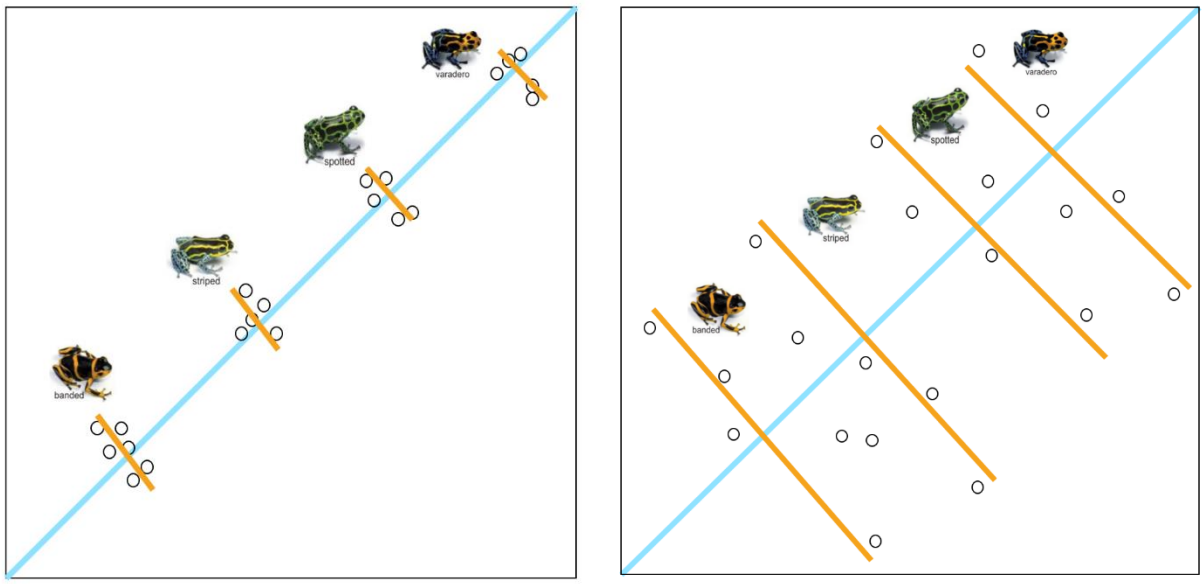

Figure 5. Left: The between group variance (blue) is greater than within group variance (orange), so the color morphs belong to statistically different groups in this theoretical model. Right: within group variance (orange) is greater than between group variance (blue), so the morphs do not belong to statistically different groups in this theoretical model.

One-way ANOVA tests were followed up by Tukey's Studentized Range (HSD) test. Whereas the F-values and P-values generated by one-way ANOVA tests merely allowed us to support or reject the null hypothesis that all color morphs belong to the same statistical group, Tukey's Studentized Range test performed pairwise comparisons to quantify the differences in mean between groups and indicated which groups were statistically different and which were not (S1 – S6).

Limitations

Several limitations exist in the methodology outlined above. The most significant limitations are: microscope magnification power, an inability to identify pigments inside chromatophores, and a degree of subjectivity in classifying skin sections as yellow, orange, or green.

The brightfield microscope used in this study had significantly less magnification power than the electron microscope used in some similar studies of other types of amphibian skin (Andrade 2019, Dushane 1935, Frost 1984, Stuckert 2019). The magnification power offered by the brightfield microscope did not reveal subcellular structures like vesicles or crystal platelets inside chromatophores. Some studies have suggested that the size and aggregation of vesicles within chromatophores has a significant effect on skin color, with brighter colors being typified by larger more aggregated vesicles (Frost 1984, Posso-Terranova 2017). Likewise, the width and orientation of guanine platelets in iridophores may influence skin color (Stuckert 2019, Twomey 2020). Iridophores themselves, generally found between xanthophore layers and melanophore layers, could not be confidently identified under the brightfield microscope. As a supplemental measure, results from previous TEM studies of *R. imitator* skin were compared to the results obtained by the present study in the discussion section.

Chromatophores can contain various types of pigments, described in Table 2. The type of pigment found in a chromatophore has a significant influence on skin color. The present study lacks data on the pigment types contained by the skin sections used to prepare the histological slides. Without pigment characterization or magnification power allowing for differentiation between pigment vesicles, the present study cannot determine the relative influence of pigment type vs. cell type on skin color. However, our results can be used to corroborate observations from

previous studies in which pigment type was characterized prior to the construction of histological slides.

Chromatophore	Pigment	Color produced
Melanophore	Pheomelanin	yellow-browns
	Eumelanin	dark browns and blacks
Xanthophore	Carotenoids	oranges and reds
	Pteridines	yellows and oranges
Iridophore	NA	NA

Table 2. Pigments found inside chromatophores and the colors they produce.

Finally, many of the colors observed in this study exist along a gradient. During skin sectioning, a standardized color wheel was used to place skin sections in the appropriate color category. However, the boundary lines between colors were potentially subject to human perceptual bias.

Results

Black skin

All morphs of *R. imitator* exhibit a dark black dorsal background against which bands of color are presented. Black skin from all morphs was typified by a thick band of melanophores directly below the epidermis and a complete lack of other types of chromatophores. Finger-like projections of melanophores were observed surrounding poison glands. The results of the ANOVA suggest no statistically significant differences in melanophore abundance in black skin tissue from the striped, spotted, or banded morphs. However, the varadero morph was statistically different from the other three morphs, with approximately 3% less melanophore abundance than the other morphs (S1).

Although some polymorphic dendrobatids do exhibit dorsal backgrounds of varying darkness, the pressure for *R. imitator* morphs to resemble their models (all of which exhibit dark dorsal backgrounds) would seem to conserve the dark dorsal background trait within the species, and no difference in background color has previously been described (Posso-Terranova 2017). Therefore, it is unsurprising that melanophore abundance in black skin tissue does not vary between three of the four color morphs. The outlying varadero morph exhibits the smallest area of black skin on its dorsum, and one previous study found that varadero tadpoles have significantly lower expression of the *mitf* gene, which encodes the melanogenesis associated transcription factor (Stuckert 2020). A downregulation of melanogenesis in varadero tadpoles would be consistent with a decrease in melanophore abundance in adult varadero frogs.

Yellow and orange skin

Of the four morphs of *R. imitator*, three exhibit patches of yellow or orange skin. The striped morph exhibits yellow skin, and the banded and varadero morphs exhibit orange skin. (The spotted

morph does not exhibit yellow or orange skin). Yellow and orange skin tissue sections were typified by a thin layer of xanthophores located directly below the epidermis and directly above the melanophore layer. At the level of magnification used in this project, the boundary between the xanthophore and melanophore layers appeared discrete and was not characterized by projections of melanophores into the xanthophore layer.

The results of the ANOVA suggest a statistically significant difference in the abundance of xanthophores in yellow/orange tissue from the banded and striped morphs ($\bar{x}_{banded\text{-}striped}$ = 5.6480) and the banded and varadero morphs ($\bar{x}_{banded\text{-}varadero}$ = 4.7306). However, there was no significant difference between the varadero and striped morphs (S2). The abundance of melanophores in yellow and orange skin sections was also found to be significantly different across all three color morphs, with the striped morph exhibiting the greatest abundance of xanthophores, followed by the varadero morph, then the banded morph (S3).

A previous comparison of spectral reflectance across the four color morphs of *R. imitator* found that the banded morph exhibits the brightest and most high contrast colors (Twomey 2016). In the present study, the banded morph was found to contain the greatest number of xanthophores and the fewest number of melanophores in orange skin tissue, which may be consistent with the production of bright colors. The striped morph exhibited the least abundance of xanthophores, which may indicate that fewer carotenoid/pteridine pigments are required to produce yellow colors than orange colors.

Green skin

Of the four morphs of *R. imitator,* two exhibit green skin: the striped morph and the spotted morph. Green skin sections were characterized by a thin layer of xanthophores directly below the

epidermis and above the melanophore layer. Presumably, iridophores were also present in green skin tissue, but they were not detectable at the magnification level used in this project.

The one-way ANOVA test suggests a significant difference in the abundance of both xanthophores and melanophores between green skin sections and the previously examined orange skin sections. Both xanthophore and melanophore abundance also show significant differences between the two morphs exhibiting green skin tissue: the striped and spotted morphs (S4, S5).

Both frogs capable of producing green coloration exhibit a lower abundance of xanthophores ($\bar{x}_{striped} = 5.832$, $\bar{x}_{spotted} = 2.117$) than frogs exhibiting orange colors ($\bar{x}_{varadero} = 7.212$, $\bar{x}_{banded} = 11.942$), which suggests that the production of green coloration may depend less on contributions from carotenoid and pteridine pigments and more on contributions from unquantified subcellular structures. Frogs capable of producing green coloration also exhibit a higher abundance of melanophores ($\bar{x}_{striped} = 11.672$, $\bar{x}_{spotted} = 17.276$) than frogs that produce orange coloration ($\bar{x}_{varadero} = 7.868$, $\bar{x}_{banded} = 5.808$). Previous studies have proposed that melanophore layers may be thickened below iridophores to absorb light that is scattered randomly by the guanine platelets, which may explain the increased melanophore abundance in green skin (Shawkey 2017).

A previous comparison of spectral reflectance across the four color morphs of *R. imitator* found that the spotted morph exhibits the least bright and lowest contrast colors (Twomey 2020). In the present study, the spotted morph was found to contain the lowest abundance of xanthophores and the greatest abundance of melanophores in colored skin tissue, forming an inverse relationship with the banded morph, which exhibits the brightest and most high contrast colors. Together, these results suggest that a high ratio of xanthophores to melanophores may produce bright colors, whereas a low ratio of xanthophores to melanophores may produce dull colors.

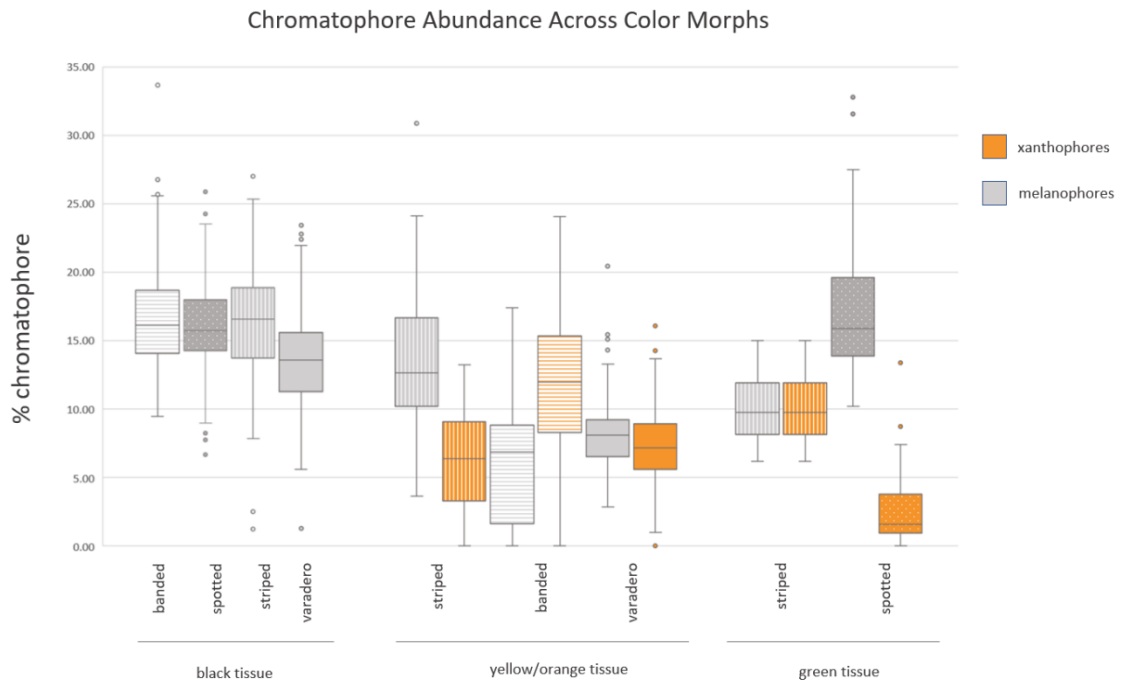

Figure 6. Summary of results from measurements of chromatophores across color morphs. Few significant differences exist in black skin tissue across color morphs. In yellow/orange skin tissue, the striped (yellow) morph exhibits lesser xanthophore abundance and greater melanophore abundance than the banded or varadero (orange) morphs. In green skin tissue, the spotted morph exhibits lesser xanthophore abundance and greater melanophore abundance than the striped morph. The morph with brightest colors (banded morph) has the highest ratio of xanthophores to melanophores and that the morph with the dullest colors (spotted morph) has the lowest ratio of xanthophores to melanophores. Tests of statistical significance can be found in S1 – S5.

Poison glands

Like other dendrobatid frogs, all morphs of *R. imitator* have specialized glands in the integumentary system from which sequestered toxins can be released. In the skin sections collected for this project, the poison glands appeared as round regions of tissue containing empty vesicles

and spanning from the dermis to the epidermis. Melanophores often wrapped around the perimeters of the glands.

The results of the one-way ANOVA test suggest a statistically significant difference in the abundance of glands in skin tissue from three of the four color morphs, with the varadero morph exhibiting the greatest abundance of glands ($\bar{x}_{varadero} = 10.438$) and the spotted and banded morphs exhibiting no significant differences and tying for least abundance of glands ($\bar{x}_{spotted} = 4.593$, $\bar{x}_{banded} = 4.466$) (S6).

DISCUSSION

The results of this study, supplemented with previously published literature, can be used to address several questions. First, are significant histological differences present in the integumentary system of *R. imitator* frogs of different color morphs? (The answer to this question is, demonstrably, yes). Second, can the observed histological differences be associated with the timing of divergence of color morphs? Additionally, comparison of poison gland abundance across color morphs may help to evaluate conflicting hypotheses that attempt to explain the mechanisms behind variation in toxicity in poison frogs and the quantitative honesty of aposematic signals in poison frogs.

Histological differences and timing of divergence

Several previous Summers' lab members have studied the timing of divergence between color morphs and the current rates of gene flow between populations of different color morphs. In 2016, Evan Twomey tested thirty-one possible topologies for a Bayesian tree mapping divergence between the color morphs and found strong support for a single, most likely tree (Twomey 2016). That tree finds an initial divergence between the varadero and banded morphs, followed by a divergence between the varadero and striped morphs, and finally a divergence between the striped and spotted morphs. Gene flow persists between the striped, spotted, and banded morphs (Twomey 2016).

The present study conducted Tukey's Studentized Range tests to compare histological differences between color morphs. For melanophore abundance in black skin, three out of the four color morphs showed no significant difference. However, for both xanthophore and melanophore abundance in yellow/orange skin, the greatest histological differences were observed between the

striped and banded morphs, followed by the banded and varadero morphs. The striped and varadero morphs were the most similar. (The spotted morph was excluded from this comparison because it did not exhibit any yellow or orange skin). This pattern roughly follows the divergence history reported in Twomey 2016, with the striped and banded morphs being the most distantly related, and the banded and varadero and striped and varadero morphs sharing recent common ancestors (Twomey 2016).

Histological differences between xanthophore and melanophore abundance in green skin cannot be ranked across color morphs because only two morphs exhibit green skin: the spotted and striped morphs. However, it is noteworthy that Twomey 2016 found the spotted and striped morphs to make up the most recent divergence in the *R. imitator* complex, so their unique green skin (and the histological structures that produce it) may be considered a synapomorphy of the group (Twomey 2016).

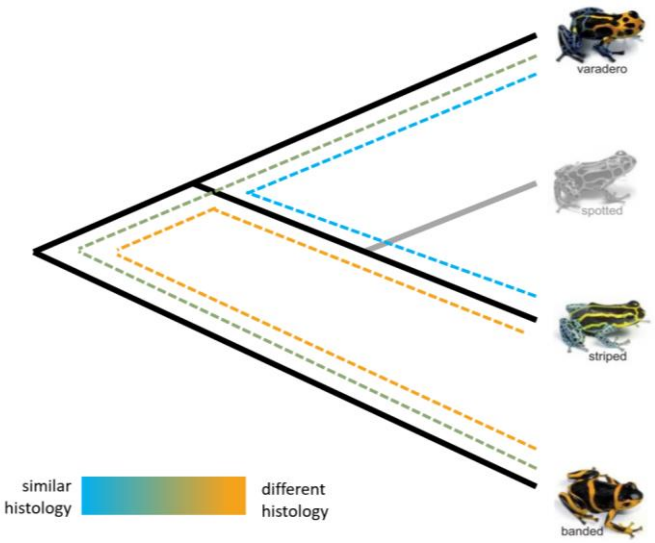

Figure 7. The abundance of xanthophores and melanophores in yellow/orange skin tissue from the varadero, striped, and banded morphs corresponds to the divergence pattern proposed by Twomey

2016. The spotted morph was excluded from this comparison because it lacked yellow/orange skin tissue. However, it shares green skin as a synapomorphy with the striped morph.

With the exclusion of melanophore abundance in black skin, histological differences between the *R. imitator* color morphs appear to support the temporal pattern of divergence reported by Twomey 2016. Importantly, histological similarities between the color morphs cannot be attributed to recent gene flow, as the most histologically similar morphs (varadero and striped) do not experience significant rates of gene flow, whereas some populations of the most histologically different morphs (striped and banded) do experience significant rates of gene flow (Twomey 2013). Instead, as evolutionary time passes between divergence events, histological differences accumulate, making each morph progressively less similar to the other morphs. This accumulation of differences is consistent with speciation at an early stage.

Poison gland abundance and alkaloid content

A study of the alkaloid content of all four morphs of *R. imitator* and their model species was published by previous Summers lab member Adam Stuckert (Stuckert 2014). The spotted morph contained the greatest quantities of alkaloids, followed by the striped morph, then the banded and varadero morphs, which were not statistically different from each other (Stuckert 2014). The present study found the greatest abundance of glands in skin sections taken from the varadero morph, followed by the striped morph, then the spotted and banded morphs, which were not statistically different from each other.

Previous studies have speculated that variations in toxicity across color morphs of polymorphic frogs could be attributed either to 1) genetic adaptations allowing some frogs to

sequester more toxins than others or 2) differences in the diets available to frogs in dispersed populations. The present study found that the varadero morph may be anatomically equipped to sequester more toxins than other *R. imitator* morphs. However, a field study found that the varadero morph carries the least amount of alkaloid defenses, compared to other morphs (Stuckert 2014). This discrepancy suggests that the strength of a frogs' defenses may be more related to available diet than to anatomical capacity for sequestering toxins. An exception to this rule may be found in certain frogs who have the ability to metabolically alter alkaloids after ingestion, making their toxins more potent and their defenses stronger (Daly 2003, Saporito 2006).

Hypothesis…	**Discussed in…**	**Current findings…**
Toxicity level is constrained by poison gland size/abundance	Stynoski and O'Connell 2017, Saporito 2010	Support only during early development. As adults, the morph with the greatest abundance of poison glands (varadero) exhibits the lowest alkaloid content in the wild
Toxicity level depends on dietary availability of carotenoids	Saporito 2006	Support. In the wild, the varadero morph contains the lowest quantities of alkaloids despite having the greatest abundance of glands, which suggests that their toxicity levels are constrained by dietary availability
Toxicity level depends on metabolic conversion of alkaloids	Daly 2003, Saporito 2006	Neither support nor fail to support
Cryptic color morphs sequester more toxins than aposematic conspecifics	Yang 2019	Do not support. The brightest morph (banded) and the dullest morph (spotted) showed no statistical difference in poison gland abundance
Individuals within a color morph show no correlation between color intensity and toxicity level	Stuckert 2018	Support for morphs, which may extend to individuals within morphs. The brightest morph (banded) and the dullest morph (spotted) showed no statistical difference in poison gland abundance

Table 3. Hypotheses related to variation in toxicity among dendrobatids and the implications of our results on those hypotheses.

Additionally, previous studies have demonstrated that the banded morph exhibits the brightest and most high contrast colors of all the *R. imitator* color morphs, whereas the striped morph exhibits the dullest and least contrasting colors (Twomey 2013). Our results show no significant difference between the abundance of poison glands in the banded and spotted morphs, which suggests that there is no anatomical basis for the banded morph to have a higher level of toxicity than the spotted morph. Therefore, in the case of *R. imitator,* intraspecific color variation does not seem to reflect a quantitatively honest aposematic signal.

Conclusions

Color pattern has been proposed as a 'magic trait' in the mimic poison frog, *Ranitomeya imitator*. To qualify as a magic trait, color pattern must be subject to natural selection, responsible for assortative mating, and associated with speciation at an early stage. The present study demonstrates that differences in the proximal mechanisms of color production have accumulated in the four color morphs of *R. imitator* since they diverged from each other. The most recently diverged morphs have the most similar histology, whereas morphs who diverged in the distant past have significant histological differences. This pattern is consistent with early-stage speciation and joins the body of evidence supporting the hypothesis that color pattern is a magic trait in *R. imitator* and, more broadly, that color polymorphism can be seen as an ecological indicator of speciation.

Future directions

As noted in the limitations section, no data was available about the subcellular structures (pigment vesicles and reflective platelets) contained within the chromatophores measured in this study. Since different pigments can be found in the same type of chromatophore, it's possible that some variation in coloration may be more properly attributed to pigment identity than chromatophore abundance. For example, it's possible that a frog with relatively few xanthophores may still be able to produce a bright orange coloration if those xanthophores contain the pigment drosopterin rather than sepiapterin. Likewise, the angle, width, and dispersion of reflective platelets in iridophores has been shown to lead to reflection of different wavelengths of light (Shawkey 2005, Shawkey 2017). Thus a frog with relatively few xanthophores underlaid by a thick layer of iridophores reflecting orange light may be capable of producing a bright orange color. Fortunately, a thorough study of the subcellular structures responsible for creating color pattern in *R. imitator* was recently published by a previous Summers lab member, Evan Twomey, and should be considered an important counterpart to this study (Twomey 2020).

In the present study, a one-way ANOVA test was used to measure differences in chromatophore abundance between skin sections of known origin. While the ANOVA test did produce statistically significant results, a further test of the explanatory power that chromatophore abundance has over color morph would be to develop a predictive model and test the model's ability to correctly identify the origins of unknown skin samples.

Finally, the majority of studies of color pattern in dendrobatid frogs to date have taken advantage of natural variation in the study system rather than undertaking experimental manipulation of the study system. In the future, it would interesting to see if experimental manipulation of dendrobatid frogs could cause some of the effects we are currently only able to

correlate with mechanisms. For example, the present study found that the spotted morph had a much lower abundance of xanthophores in its green tissue than the banded morph had in its orange tissue. Previous studies have identified *pax7* and *xdh* as genes associated with the early development of xanthophores and have found both genes to be differentially expressed across the color morphs of *R. imitator* during development (Stuckert 2020). If the *pax7* and/or *xdh* gene could be overexpressed in spotted *R. imitator* embryos and the overexpression of those genes led to adult spotted frogs with more abundant xanthophores and a more orange color pattern, then there would be evidence that increasing xanthophore abundance causes orange skin rather than merely being correlated with it.

References

1. Alho J, Herczeg G, Soderman F, Laurila A, Jonsson K, Merila J. 2010. Increasing melanin along a latitudinal gradient in a widespread amphibian: local adaptation, ontogenic, or environmental plasticity? Evolutionary Biology **10:** 317 – 322.
2. Andrade P, et al. 2019. Regulatory changes in pterin and carotenoid genes underlie balanced color polymorphisms in the wall lizard. Proceedings of the National Academy of Sciences **116:** 5633 – 5642.
3. Bagnara JT, Taylor JD, Hadley ME. 1968. The dermal chromatophore unit. Journal of Cell Biology **38:** 67 – 79.
4. Benitez M, Del Pino EM. 2002. Expression of brachyury during development of the dendrobatid frog *Colostethus machalilla.* Developmental Dynamics **225:** 592 – 596.
5. Bond A. 2007. The evolution of color polymorphism: Crypticity, searching images, and apostatic selection. Annual Review of Ecological and Evolutionary Systems **38**: 489–514.
6. Braasch, I, Schartl M, Volff J. 2007. Evolution of pigment synthesis pathways by gene and genome duplication in fish. BMC Evolutionary Biology **7:** 74 – 92.
7. Brooks O, Saporito R. 2019. For poison frogs, bitter is better. Biochemist **41:** 16-20.
8. Caldwell J, Myers C. 1990. A new poison frog from Amazonian Brazil, with further revision of the quinquevittatus group of dendrobates. American Museum Novitiates **2998**: 1 – 21.
9. Daly JW, Garraffo HM, Spande TF, Clark VC, Ma J, Ziffer H, Cover JF. 2003. Evidence for an enantioselective pumiliotoxin 7-hydroxylase in dendrobatid poison frogs of the genus Dendrobates. Proceedings of National Academy of Sciences USA **100**: 11092–11097.

10. DuShane GP. 1935. An experimental study of the origin of pigment cells in Amphibia. Experimental Zoology **72:** 1 – 31.
11. Ford E. 1945. Polymorphism. Biology Review. **20**: 73–88.
12. Frost S, Robinson SJ. 1984. Pigment cell differentiation in the fire-bellied toad, *Bombina orientalis*. Journal of Morphology **179:** 229 – 242.
13. Gallant J, et al. 2014. Ancient homology underlies adaptive mimetic diversity across butterflies. Nature Communications **5:** 4817 – 4827.
14. Gray S, McKinnon J. 2007. Linking color polymorphism maintenance and speciation. Trends in Ecology and Evolution **22:** 71–79.
15. Mckinnon J, Pierotti, M. 2010. Colour polymorphism and correlated characters: Genetic mechanisms and evolution. Molecular Ecology **19**: 5101–5125.
16. McLean C, Stuart-Fox D. 2014. Geographic variation in animal colour polymorphisms and its role in speciation. Biology Reviews **89:** 860–873.
17. Mills M, Patterson LB. 2008. Not just black and white: pigment pattern development and evolution in vertebrates. Seminars in Cell and Developmental Biology **20:** 72 – 81.
18. Nielsen R. 2005. Molecular signatures of natural selection. Annual Review of Genetics **39**: 197 – 218.
19. Posso-Terranova A, Andres J. 2017. Diversification and convergence of aposematic phenotypes: truncated receptors and cellular arrangements mediate rapid evolution of harlequin poison frogs. Evolution **71:** 2677 – 2692.
20. Posso-Terranova A, Andres J. Genetic bases of aposematic traits: insights from the skin transcriptional profiles of *Oophaga* poison frogs. In review.

21. Reynolds R, Fitzpatrick B. 2007. Assortative mating in poison-dart frogs based on an ecologically important trait. Evolution **61** DOI 10.1111/j.1558-5646.2007.00174.x
22. Saporito R, Donnelly MA, Garraffo MH, Spande TF, Daly JW. 2006. Geographic and seasonal variation in alkaloid-based chemical defenses of *Dendrobates pumilio* from Bocas del Toro, Panama. Journal of Chemical Ecology **32:** 795-814.
23. Segami Marzal J, Rudh A, Rogell B, Odeen A, Lovlie H, Rosher C, Qvarnstrom A. 2017. Cryptic female Strawberry poison frogs experience elevated predation risk when associating with an aposematic partner. Ecology and Evolution **7** DOI 10.1002/ece3.2662
24. Servedio MR, Sander van Doorn G, Kopp M, Frame AM, Nosil P. 2011. Magic traits in speciation: 'magic' but not rare? Trends in Ecology and Evolution **26:** 389 – 397.
25. Shawkey M, d'Alba L. 2017. Interactions between colour-producing mechanisms and their effects on the integumentary colour palette. Philosopical Transactions of the Royal Society B **372:** 20160536.
26. Shawkey M, Hill G. 2005. Carotenoids need structural colours to shine. Biology Letters **1**: 121–124.
27. Stuart-Fox D, Rankin K, Lutz A, Elliott A, Hugall A, McLean C, Medina I. 2021. Environmental gradients predict the ratio of environmentally acquired carotenoids to self-synthesized pteridine pigments. Ecological Letters **24:** 2207-2218.
28. Stuckert AM, Linderoth T, MacManes M, Summers K. Differential gene expression and gene variants drive color and pattern development in divergent color morphs of a mimetic poison frog. In review.
29. Stuckert AM, Moore E, Coyle KP, Davison I, MacManes M, Roberts R, Summers K. 2019. Variation in pigmentation gene expression is associated with distinct aposematic color

morphs in the poison frog *Dendrobates auratus*. BMC Evolutionary Biology **19** 10.1186/s12862-019-1410-7.

30. Stuckert AM, Saporito R, Summers K. 2018. An empirical test indicates only qualitatively honest aposematic signaling within a population of vertebrates. Journal of Herpetology **52:** 201-208.
31. Stuckert AM, Saporito R, Venegas P, Summers K. 2014. Alkaloid defenses of co-mimics in a putative Mullerian mimetic radiation. BMC Evolutionary Biology **14** DOI 10.1186/1471-2148-14-76
32. Stuckert AM, Venegas PJ, Summers K. 2014. Experimental evidence for predator learning and Mullerian mimicry in Peruvian poison frogs. Evolutionary Ecology **28**: 413 – 426.
33. Stynoski J, O'Connell L. 2017. Developmental morphology of granular skin glands in pre-metamophic egg-eating frogs. Zoomorphology **136:** 219 – 224.
34. Summers K, Clough M. 2001. The evolution of coloration and toxicity in the poison frog family (Dendrobatidae). Proceedings of the National Academy of Science **98:** 6227-6232.
35. Symula R, Schulte R, Summers K. 2001. Molecular phylogenetic evidence for a mimetic radiation in Peruvian poison frogs supports a Mullerian mimicry hypothesis. Proceedings of the Royal Society B **268** DOI 10.1098/rspb.2001.1812.
36. Twomey E, Kain M, Claeys M, Summers K, Castroviejo-Fisher S, Bocxlaer IV. 2020. Mechanisms for color convergence in a mimetic radiation of poison frogs. The American Naturalist **195** DOI 10.1086/708157
37. Twomey E, Vestergaard JS, Summers K. 2014. Reproductive isolation related to mimetic divergence in the poison frog *Ranitomeya imitator*. Nature Communications **5** DOI: 10.1038/ncomms5749.

38. Twomey E, Vestergaard JS, Venegas PJ, Summers K. 2016. Mimetic divergence and the speciation continuum in the mimic poison frog *Ranitomeya imitator*. The American Naturalist **187** DOI 10.1086/684439.

39. Twomey E, Yeager J, Brown JL, Morales V, Cummings M, Summers K. 2013. Phenotypic and genetic divergence among poison frog populations in a mimetic radiation. PLOS One **8** DOI 10.1371/journal.pone.0055443.

40. Vestergaard J, Twomey E, Larsen R, Summers K, Nielsen R. 2015. Number of genes controlling a quantitative trait in a hybrid zone of the aposematic frog *Ranitomeya imitator.* Proceedings of the Royal Society B **282** DOI 10.1098/rspb.2014.1950.

41. Wang I, Shaffer HB. 2008. Rapid color evolution in an aposematic species: a phylogenetic analysis of color variation in the strikingly polymorphic strawberry poison-dart frog. Evolution **62:** 2742-2759.

42. Wellenreuther M, Svensson E, Hansson B. 2014. Sexual selection and genetic colour polymorphisms in animals. Molecular Ecology **23**: 5398–5414.

43. White T, Kemp D. 2016. Quick guide: color polymorphism. Current Biology **26:** 515 – 522.

44. Yang Y, Servedio M, Richards-Zawaki C. 2019. Imprinting sets the stage for speciation. Nature Letters **574:** 99 – 112.

45. Yeager J, Brown J, Morales V, Cummings M, Summers K. 2012. Testing for selection on color and pattern in a mimetic radiation. Current Zoology **58:** 668 – 676.

Appendix A: Supplemental List

Supplemental 1. Tukey's Studentized Range (HSD) test for the percentage of melanophores found in black skin tissue.

S1. Melanophore Abundance in Black Skin Tissue				
A one-way ANOVA test with 3 degrees of freedom produced an F-value of 51.96 and a $P_r > F$ of > .0001. Tukey's HSD test with 5 degrees of freedom and an alpha of 0.05 produced the following results…				
Morph Comparison	**Difference Between Means**	**Simultaneous 95% Confidence Limits**		**Significance**
banded - striped	0.0189	-0.6838	0.7215	
banded - spotted	0.4213	-0.3060	1.1486	
banded - varadero	2.8075	2.1133	3.5017	***
striped - banded	-0.0189	-0.7215	0.6838	
striped - spotted	0.4024	-0.3087	1.1135	
striped - varadero	2.7886	2.1114	3.4658	***
spotted - banded	-0.4213	-1.1486	0.3060	
spotted - striped	-0.4024	-1.1135	0.3087	
spotted - varadero	2.3862	1.6834	3.0890	***
varadero - banded	-2.8075	-3.5017	-2.1133	***
varadero - striped	-2.7886	-3.4658	-2.1114	***
varadero - spotted	-2.3862	-3.0890	-1.6834	***

Supplemental 2. Tukey's Studentized Range (HSD) test for the percentage of xanthophores found in yellow (striped) and orange (banded and varadero) skin tissue.

S2. Xanthophore Abundance in Yellow/Orange Skin Tissue				
A one-way ANOVA test with 2 degrees of freedom produced an F-value of 99.37 and a $P_r > F$ of > .0001. Tukey's HSD test with 5 degrees of freedom and an alpha of 0.05 produced the following results…				
Morph Comparison	**Difference Between Means**	**Simultaneous 95% Confidence Limits**		**Significance**
banded - varadero	4.7306	3.8730	5.5882	***
banded - striped	5.6480	4.2457	7.0502	***
varadero - banded	-4.7306	-5.5882	-3.8730	***
varadero - striped	0.9174	-0.4665	2.3014	

striped - banded	-5.6480	-7.0502	-4.2457	***
striped - varadero	-0.9174	-2.3014	0.4665	

Supplemental 3. Tukey's Studentized Range (HSD) test for the percentage of melanophores found in yellow (striped) and orange (banded and varadero) skin tissue.

S3. Melanophore Abundance in Yellow/Orange Skin Tissue				
A one-way ANOVA test with 2 degrees of freedom produced an F-value of 109.57 and a $P_r >$ F of > .0001. Tukey's HSD test with 5 degrees of freedom and an alpha of 0.05 produced the following results…				
Morph Comparison	**Difference Between Means**	**Simultaneous 95% Confidence Limits**		**Significance**
banded - varadero	-2.0605	-2.8194	-1.3016	***
banded - striped	7.7641	6.5233	9.0050	***
varadero - banded	2.0605	1.3016	2.8194	***
varadero - striped	-5.7037	-6.9283	-4.4791	***
striped - banded	7.7641	6.5233	9.0050	***
striped - varadero	5.7037	4.4791	6.9238	***

Supplemental 4. Tukey's Studentized Range (HSD) test for the percentage of xanthophores found in green (spotted and striped) and orange (banded and varadero) skin tissue. Note that the striped samples in S4 are not the same as the striped samples in S2 and S3; they are green tissue rather than yellow.

S4. Xanthophore Abundance in Green/Orange Skin Tissue				
A one-way ANOVA test with 3 degrees of freedom produced an F-value of 195.13 and a $P_r >$ F of > .0001. Tukey's HSD test with 5 degrees of freedom and an alpha of 0.05 produced the following results…				
Morph Comparison	**Difference Between Means**	**Simultaneous 95% Confidence Limits**		**Significance**
banded - striped	6.1097	5.0311	7.1883	***
banded - spotted	9.8250	8.7272	10.9227	***
banded - varadero	4.7306	3.8529	5.6082	***
striped - banded	-6.1097	-7.1883	-5.0311	***

striped - spotted	3.7153	2.4725	4.9581	***
striped - varadero	-1.3791	-2.4326	-0.3256	***
spotted - banded	-9.8250	-10.9227	-8.7272	***
spotted - striped	-3.7153	-4.9851	-2.4725	***
spotted - varadero	-5.0944	-6.1676	-4.0213	***
varadero - banded	-4.7306	-5.6082	-3.8529	***
varadero - striped	1.3791	0.3256	2.4326	***
varadero - spotted	5.0944	4.0213	6.1676	***

Supplemental 5. Tukey's Studentized Range (HSD) test for the percentage of melanophores found in green (spotted and striped) and orange (banded and varadero) skin tissue. Note that the striped samples in S5 are not the same as the striped samples in S2 and S3; they are green tissue rather than yellow.

S5. Melanophore Abundance in Green/Orange Skin Tissue				
A one-way ANOVA test with 3 degrees of freedom produced an F-value of 261.98 and a $P_r >$ F of > .0001. Tukey's HSD test with 5 degrees of freedom and an alpha of 0.05 produced the following results…				
Morph Comparison	**Difference Between Means**	**Simultaneous 95% Confidence Limits**		**Significance**
banded - striped	-5.8648	-6.9636	-4.7660	***
banded - spotted	-11.4690	-12.5873	-10.3507	***
banded - varadero	-2.0605	-2.9546	-1.1664	***
striped - banded	-6.1097	-7.1883	-5.0311	***
striped - spotted	-5.6042	-6.8703	-4.3381	***
striped - varadero	3.8043	2.7311	4.8776	***
spotted - banded	5.8648	4.7660	6.9636	***
spotted - striped	5.6042	4.3381	6.8703	***
spotted - varadero	9.4085	8.3153	10.5018	***
varadero - banded	2.0605	1.1664	2.9546	***
varadero - striped	-3.8043	-4.8776	-2.7311	***
varadero - spotted	-9.4085	-10.5018	-8.3153	***

Supplemental 6. Results of Tukey's Studentized Range test for poison gland abundance.

S6. Poison Gland Abundance				
A one-way ANOVA test with 3 degrees of freedom produced an F-value of 86.81 and a $P_r > F$ of > .0001. Tukey's HSD test with 5 degrees of freedom and an alpha of 0.05 produced the following results…				
Morph Comparison	**Difference Between Means**	**Simultaneous 95% Confidence Limits**		**Significance**
banded - striped	-5.8648	-6.9636	-4.7660	***
banded - spotted	-11.4690	-12.5873	-10.3507	
banded - varadero	-2.0605	-2.9546	-1.1664	***
striped - banded	-6.1097	-7.1883	-5.0311	***
striped - spotted	2.4327	1.2008	3.6646	***
striped - varadero	-3.4124	-4.5320	-2.2929	***
spotted - banded	2.5600	1.4012	3.7187	
spotted - striped	5.6042	4.3381	6.8703	***
spotted - varadero	-5.8451	-7.0025	-4.6877	***
varadero - banded	5.9724	4.8931	7.0516	***
varadero - striped	3.4124	2.2928	4.5320	***
varadero - spotted	5.8451	4.6877	7.0025	***